DMD Fast Forward. Published on February 26, 2016 as DOI: 10.1124/dmd.116.069344
This article has not been copyedited and formatted. The final version may differ from this version.

Role of Chromatin Structural Changes in Regulating Human CYP3A Ontogeny

Nicholas L. Giebel, Jeffrey D. Shadley, D. Gail McCarver, Kenneth Dorko, Roberto Gramignoli, Stephen C. Strom, Ke Yan, Pippa M. Simpson and Ronald N. Hines

Departments of Pediatrics and Pharmacology & Toxicology, Medical College of Wisconsin, and Children's Research Institute, Children's Hospital and Health Systems, Milwaukee WI USA (NLG, JDS, DGM, PS, KY, RNH); Department of Pathology, University of Pittsburgh, Pittsburgh PA, USA (KD, RG, SCS)

* Current Addresses: Milwaukee WI USA (NLG); Department of Pediatrics Critical Care, University of Michigan Health System, Ann Arbor MI USA (JDS); Cary NC USA (DGM); Samsara Sciences, San Diego CA USA (KD); Department of Laboratory Medicine, Karolinska Institutet and Hospital, Stockholm Sweden (RG, SCS); U.S. Environmental Protection Agency, Office of Research and Development, National Health and Environmental Effects Research Laboratory, Research Triangle Park, NC USA (RNH)

Running Title: Chromatin Structural Changes Regulating Human CYP3A Ontogeny

Corresponding Author:

Ronald N. Hines

US Environmental Protection Agency

Office of Research and Development

National Health and Environmental Effects Research Laboratory

109 T.W. Alexander Dr., MD 305-02

Research Triangle Park NC 27711

919-541-5622

hines.ronald@epa.gov

Text pages: 36

Tables: 6

Figures: 6

References: 49

Words in Abstract: 231

Words in Introduction: 706

Words in Discussion: 1493

Non-standard abbreviations: bp(s), base pair(s); C/EBP, CCAAT/enhancer binding protein; ChIP, chromatin immunoprecipitation; CLEM4, constitutive liver enhancer module 4; C_q, quantification cycle; DME, drug metabolizing enzyme; HNF4α, hepatocyte nuclear factor 4 alpha; PXR, pregnane X receptor; qPCR, quantitative polymerase chain reaction; TBP, TATA-box binding protein; TFIID, transcription factor II D; TSS, transcription start site; USF1, upstream stimulatory factor 1; XREM, xenobiotic-response enhancer module

DMD Fast Forward. Published on February 26, 2016 as DOI: 10.1124/dmd.116.069344
This article has not been copyedited and formatted. The final version may differ from this version.

Abstract

Variability in drug metabolizing enzyme developmental trajectories contributes to interindividual differences in susceptibility to chemical toxicity and adverse drug reactions, particularly in the first years of life. Factors linked to these interindividual differences are largely unknown, but molecular mechanisms regulating ontogeny are likely involved. To evaluate chromatin structure dynamics as a likely contributing mechanism, age-dependent changes in modified and variant histone occupancy were evaluated within known *CYP3A4* and *3A7* regulatory domains. Chromatin immunoprecipitation using fetal or postnatal human hepatocyte chromatin pools followed by quantitative polymerase chain reaction DNA amplification was used to determine relative chromatin occupancy by modified and variant histones. Chromatin structure representing a poised transcriptional state (bivalent chromatin), indicated by the occupancy by modified histones associated with both active and repressed transcription, was observed for *CYP3A4* and most *3A7* regulatory regions in both postnatal and fetal livers. However, the *CYP3A4* regulatory regions had significantly greater occupancy by modified histones associated with repressed transcription in the fetal liver. Conversely, some modified histones associated with active transcription exhibited greater occupancy in the postnatal liver. *CYP3A7* regulatory regions also had significantly greater occupancy by modified histones associated with repressed transcription in the fetus. The occupancy by modified histones observed is consistent with chromatin structural dynamics contributing to CYP3A4 ontogeny, although the data is less conclusive regarding CYP3A7. Interpretation of the latter data may be confounded by cell-type heterogeneity in the fetal liver.

DMD Fast Forward. Published on February 26, 2016 as DOI: 10.1124/dmd.116.069344
This article has not been copyedited and formatted. The final version may differ from this version.

Introduction

CYP3A is one of the most important drug metabolizing enzyme (DME) subfamilies. The two major postnatal forms, CYP3A4 and 3A5, account for the metabolism of approximately 50% of commonly prescribed drugs that undergo oxidative transformation (Williams *et al.*, 2004). *CYP3A*s are found within a four-gene cluster consisting of *CYP3A4*, *3A5*, *3A7*, and *3A43* (Plant, 2007). Although the CYP3A subfamily members share a high degree of amino acid and DNA sequence identity, their tissue- and age-specific expression patterns and substrate specificities are considerably different (de Wildt *et al.*, 1999). These properties are particularly evident for hepatic CYP3A4 and 3A7. CYP3A7 is present at high levels within the fetal liver, but by one to two years after birth, it is expressed at low or non-detectable levels (Stevens *et al.*, 2003). In contrast, human hepatic CYP3A4 is expressed at low levels beginning with the second or third trimester. Expression increases substantially after birth, and mature CYP3A4 levels are reached by one to two years of age. The clinical importance of such differential DME developmental trajectories has been repeatedly demonstrated through historical therapeutic misadventures that resulted in unexpected morbidity and mortality in pediatric patients (Hines, 2008).

Greater understanding of DME ontogeny has allowed incorporation of age-dependent changes in enzyme-specific content into physiologically based pharmacokinetic models and improved prediction of pediatric drug and toxicant disposition (Alcorn and McNamara, 2008). However, activity during the first year of life remains highly unpredictable due to differences in enzyme developmental trajectories that result in windows of hypervariability. Adding to uncertainty, the length of this hypervariable period varies from one enzyme to another (Hines, 2008). Although these hypervariable windows likely are linked to variability in the molecular mechanisms controlling enzyme ontogeny (Schuetz, 2004; Perera *et al.*, 2009; Klein *et al.*, 2012), those regulatory mechanisms remain largely unknown.

Several possible mechanisms may contribute to the dramatic changes in CYP3A4 and 3A7 that occur in the first couple years after birth. The first is differential transcription factor

DMD Fast Forward. Published on February 26, 2016 as DOI: 10.1124/dmd.116.069344
This article has not been copyedited and formatted. The final version may differ from this version.

binding within the promoters, which has been the predominant focus of previous studies (Riffel *et al.*, 2009; Matsumura *et al.*, 2004; Saito *et al.*, 2001; Ourlin *et al.*, 1997). These studies elucidated the transcription factor binding differences between the *CYP3A4* and *3A7* regulatory regions; however, most if not all of the identified factors are expressed during early development and unlikely account for the observed differential expression patterns (Cereghini, 1996). Given the high degree of *CYP3A4* and *3A7* DNA sequence identity (Plant, 2007) and the minimal *in vivo* validation for transcription factor-mediated differences, variation in these elements is an unlikely explanation for the substantial age-specific expression differences between these two genes.

A second possibility is that epigenetic mechanisms may play a role, particularly those controlling chromatin structure (Kiefer, 2007). Depending on the compaction of chromatin, DNA is either accessible (euchromatin) or inaccessible (heterochromatin) to the transcriptional machinery. At the foundation of chromatin structure is the nucleosome, composed of an octamer of two H2A, H2B, H3, and H4 histones around which approximately 147bp of DNA is wrapped (Zhou *et al.*, 2011). DNA accessibility can be altered through a complex network of specific histone N-terminal amino acid post-translational modifications (*e.g.*, acetylation and methylation) and/or histone variants (*e.g.*, H2A.Z). These modifications and variants can impact chromatin structure and have a role in regulating a large number of biological processes, including development (Suganuma and Workman, 2011). Comprehensive, genome-wide studies in human cells have demonstrated an association of modified and variant histone occupancy of promoters and/or enhancers that approximately correlates with transcriptional activity, which is summarized in Table 1.

Evidence for changes in chromatin occupancy by modified histones have been implicated in regulating mouse Cyp3a ontogeny (Li *et al.*, 2009), however, the mouse *Cyp3a* gene family differs from the human (Martignoni *et al.*, 2006) and whether or not a similar mechanism exists in the human is unknown. Because of the integral role modified and variant

histones have on chromatin structure, age-specific occupancy of key regulatory elements with modified and variant histones was hypothesized as a major mechanism regulating human *CYP3A4* and *3A7* ontogeny. To test this hypothesis, occupancy changes in seven histone modifications and one histone variant within the known *CYP3A4* and *CYP3A7* major promoter regulatory regions were evaluated and compared between fetal and postnatal primary hepatocytes.

DMD Fast Forward. Published on February 26, 2016 as DOI: 10.1124/dmd.116.069344
This article has not been copyedited and formatted. The final version may differ from this version.

Materials and Methods

Postnatal and Fetal Hepatocytes: Postnatal liver tissues were obtained through the Liver Tissue Procurement and Distribution System (National Institutes of Health Contract N01-DK-9-2310), and hepatocytes prepared as described (Gramignoli *et al.*, 2012). Four of these liver samples were from pediatric donors between 1 and 6 years of age (Table 2). To ensure mature CYP3A4 expression was present in each of these samples, as well as all postnatal samples, activities were determined using a commercial, cell-based assay (P450-Glo™ CYP3A4 Assay, Luciferin-IPA; Promega Corporation, Madison, WI, USA) with some modifications, as previously described (Gramignoli *et al.*, 2014). All but one of the postnatal samples exhibited CYP3A4 activity within one standard deviation of the mean activity previously determined for 75 primary hepatocyte preparations (Gramignoli *et al.*, 2014). All four pediatric samples exhibited CYP3A4 activity greater than the mean, with the youngest sample exhibiting the highest activity (greater than one standard deviation from the mean) (see Supplemental Figure 1S). These data are consistent with these four pediatric samples exhibiting mature CYP3A4 expression levels.

Livers from human fetal tissues having a gestational age between 13–22 weeks were obtained from Magee Women's Hospital, Pittsburgh, PA, after obtaining informed consent. Donor demographics are presented in Table 2. Fetal hepatocytes were prepared as described (Sharma *et al.*, 2013) except that the final cell pellet was suspended in 40 mL Eagle's minimal essential media and cell viability estimated by trypan blue exclusion (Table 2). Immediately after both postnatal and fetal hepatocyte cell preparation, the cells were treated with 1% (w/v) formaldehyde for 10 min to cross-link chromatin DNA and protein. The reaction was quenched with 0.125 M glycine and the cells frozen at −80°C until processed further. The Human Research Review Committee of the University of Pittsburgh approved protocols for postnatal and fetal liver tissue procurement and use.

DMD Fast Forward. Published on February 26, 2016 as DOI: 10.1124/dmd.116.069344
This article has not been copyedited and formatted. The final version may differ from this version.

Chromatin Preparation: Frozen cells were quickly thawed and suspended in lysis buffer 1 [50 mM HEPES-KOH, pH 7.9, 140 mM NaCl, 1 mM Na_2EDTA, 20 mM β-glycerophosphate, 10% (v/v) glycerol, 0.5% (v/v) NP-40, and 0.25% (v/v) Triton X-100] with protease and phosphatase inhibitors from Sigma-Aldrich (Saint Louis, MO), pepstatin A (1 µL/mL), phosphatase inhibitor cocktail 2 (1 µL/mL), phosphatase inhibitor cocktail 3 (0.6 µL/1x10^6 cells) and protease inhibitor cocktail consisting of leupeptin hemisulfate salt (10 µg/mL), aprotinin from bovine lung (0.6 µg/mL), antipain dihydrochloride (1 µg/mL), and 4-(2-aminoethyl) benzenesulfonyl fluoride hydrochloride (0.6 µg/mL). Cell suspensions were centrifuged at 2,400 g at 4°C for 10 min, and the supernatant fraction removed by gentle aspiration. The pellets were resuspended in lysis buffer 2 (200 mM NaCl, 1 mM Na_2EDTA, 0.5 mM EGTA, 10 mM Tris-HCl pH 7.9, and 20 mM β-glycerophosphate) containing the previously described protease and phosphatase inhibitors and the above centrifugation step repeated. The supernatant fractions were gently aspirated and discarded. The pellets were snap frozen using dry ice in methanol and stored at −80°C overnight.

The next day, pellets were resuspended in lysis buffer 3 [10 mM Tris-HCl pH 7.9, 100 mM NaCl, 1 mM Na_2EDTA, 0.5 mM Na_2EGTA, 20 mM β-glycerophosphate, 0.1% (w/v) sodium deoxycholate, and 0.5% (w/v) n-lauroyl sarcosine], containing the protease and phosphatase inhibitors described above. Samples were divided into 0.5 mL aliquots in convex bottom 2 mL microcentrifuge tubes and subsequently sonicated using a Misonix S-4000 sonicator (Farmingdale, NY) with the cup horn at 100% power for 10 pulses of 30 sec each with a 60 sec rest between pulses. Ice-cold water was circulated continuously through the cup horn to prevent sample heating. After visualization using a phase contrast microscope to ensure nuclear membrane disruption, the samples were further sonicated at 60% power for 30 pulses of 30 sec each with a 60 sec rest between pulses. Shearing efficacy was determined visually after purifying chromatin DNA as described below and fractionation by electrophoresis in a 1.5% agarose gel. Only DNA samples having a fragmentation pattern with the majority of fragments

DMD Fast Forward. Published on February 26, 2016 as DOI: 10.1124/dmd.116.069344
This article has not been copyedited and formatted. The final version may differ from this version.

between 200 and 1,000 base pairs were used for the study. To minimize variation between experiments, fetal and postnatal chromatin pools were prepared from 14 and 10 individual liver samples, respectively (Table 2), using equal DNA masses. These sheared chromatin pools were divided into aliquots and stored at −80°C until use in the experiments described below.

Chromatin Immunoprecipitation (ChIP): Each chromatin aliquot was cleared by incubating with sheared salmon sperm DNA (1µg, Eppendorf, Hauppauge, NY) for 30 min prior to immunoprecipitation. ChIP was performed using Chromatrap Pro-A Spin Columns (Porvair Filtration Group Ltd., UK) following the manufacturer's instructions (version 6, 2013). Column blocking was achieved by pre-loading the Chromatrap columns with sheared salmon sperm DNA (1 mg/mL) and bovine serum albumin (0.5 mg/mL; New England Biolabs, Ipswich, MA) and incubating for 30 min followed by centrifugation at 1,000 g for 30 sec. All antibodies raised against modified and variant histones were ChIP-validated by the vendor, Active Motif (Carlsbad, CA) and included anti-H2A.Z (39113), anti-H3Ac (39139), anti-H3K27me3 (39155), anti-H3K4me1 (39635), anti-H3K4me3 (39159), anti-H3K9me1 (39681), anti-H3K9me3 (39161), and anti-H4 pan-Ac (39925). ChIP-validated antibodies raised against specific transcription factors were supplied by Santa Cruz (Santa Cruz, CA) and included anti-USF1 (sc-229X), anti-HNF4α (sc-6557X), anti-HNF1α (sc-6547X), anti-C/EBPβ (sc-150X), and anti-TFIID (sc-273X) (raised against the full-length human TATA-box binding protein). The same lots of antibody were used for all experiments. After de-crosslinking immunoprecipitated chromatin, DNA was purified using the Qiagen PCR Purification Kit as described below. A minimum of three independent ChIP reactions were performed for all analyses with each independent reaction performed in triplicate.

Purification of Chromatin DNA: DNA/protein in the chromatin mixture was de-crosslinked by adding 5 µL 5 M sodium chloride and 75 µL nanopure water to a 20 µL aliquot followed by incubation at 95°C for 15 min. Subsequently, 10 µg RNase A was added, and the mixture was incubated at 37°C for 15 min. Afterwards, 1 µg of proteinase K was added, and the resulting

mixture was incubated at 67°C for 15 min. After centrifugation at 16,000 g for 4 min, the supernatant was removed and purified using a Qiagen PCR Purification Kit (Valencia, CA) per the manufacturer's instructions. Recovered DNA was quantified using a Hoechst-based DNA Quantitation Kit (Bio-Rad Laboratories, Hercules, CA); fluorescence was measured using a 360 nm excitation wavelength and 460 nm emission wavelength using a Bio-Rad Versafluor™ Fluorometer.

Primers: DNA amplification primers were designed using Clone Manager 9.0 (Scientific and Educational Software, Cary, NC) and Oligo 7 Primer Analysis Software (v7.15 Molecular Biology Industries, Cascade, CO) and screened with primer-BLAST (NCBI) to assure target specificity (Supplemental Table 1). Primer sets were designed to produce overlapping amplicons across each regulatory region of interest. Primers were obtained from Integrated DNA Technologies (IDT, Coralville, IA) as desalted, lyophilized pellets. Primer pellets were suspended in 10 mM Tris-HCl, 1 mM EDTA, and 10 mM NaCl, at pH 8.0 to a final primer concentration of 100 µM and stored at −20°C. Primer pair optimization was performed by temperature gradient quantitative polymerase chain reaction (qPCR) DNA amplification to determine the optimal annealing temperature. Melt curve analysis was done to assure amplicon specificity, and amplification products were fractionated by electrophoresis in 2% agarose gels alongside molecular weight standards to assure the expected product sizes (1 Kb plus, 100 bp ladder, Invitrogen, Grand Island, NY).

Quantitative Polymerase Chain Reaction (qPCR) DNA Amplification: qPCR reactions were performed using iQ SYBR Green Supermix (Bio-Rad Laboratories) following the manufacturer's instructions after scaling to a 20 µL reaction volume. Reactions were performed in triplicate in white 96-well plates (Bio-Rad Laboratories). Both postnatal and fetal chromatin pools immunoprecipitated with the same antibody were simultaneously analyzed on the same plate. qPCR DNA amplifications were performed using a CFX96 Optical Reaction Module and C1000 Thermal Cycler (Bio-Rad Laboratories). The cycling conditions were 3 min at 95°C for initial

DMD Fast Forward. Published on February 26, 2016 as DOI: 10.1124/dmd.116.069344
This article has not been copyedited and formatted. The final version may differ from this version.

denaturation, followed by 50 cycles consisting of denaturation for 10 sec at 95°C, annealing for 10 sec at the optimized primer set temperature (range 55–66°C), and extension for 20 sec at 72°C. Subsequently, a melting curve protocol was performed consisting of denaturation for 10 sec at 95°C, a hold for 30 sec at 65°C, and then 60 cycles of 30 sec increasing by 0.5°C in each cycle. In addition to the unknown samples, each plate included a control without any DNA template, as well as input DNA dilutions of 100%, 20%, 4%, 0.8%, and 0.16% relative to the mass of DNA used in each ChIP reaction. Data analysis was done using CFX96 Real-Time Manager software (version 2.1 Bio-Rad Laboratories) to determine the baseline, threshold, and melt curve peak temperature, as well as the quantification cycle (C_q). The C_q value represents the number of amplification cycles required for the fluorescence signal to be above background as a log base two function and is inversely related to the DNA template copy number.

Data Analysis: qPCR data were initially examined by plotting the relative fluorescent units on a semi-log scale to assure that threshold values were within the linear portions of the amplification curves. A modification of the delta C_q (ΔC_q) method was used to express the relative occupancy of the targeted protein on specific *CYP3A4* (NG_008421.1) or *CYP3A7* (NG_007983.1) DNA elements within the postnatal or fetal chromatin pools. Linear regression analysis of the C_q values from the input DNA dilutions was used to obtain a linear function from which the PCR amplification efficiency and a C_q value for the input DNA at 100% were calculated. Dilution curve functions with a correlation coefficient value greater than 0.98 and PCR amplification efficiency values ranging from 0.9 to 1.05 were included in the analysis. C_q values determined from qPCR analysis of DNA isolated from ChIP reactions were normalized to the calculated C_q value for 100% input DNA to obtain a ΔC_q. ΔC_q values were excluded if, based on a box and whisker plot analysis of all ChIP reactions for a single experiment, all three data points plotted as outliers (1.5-times the quartile values) (Burns *et al.*, 2005). The median ΔC_q values for chromatin occupancy by modified histones, variant histones, or transcription factors from the fetal and postnatal chromatin pools were compared using the Mann-Whitney U test. Sigmaplot 9.01 (San

DMD Fast Forward. Published on February 26, 2016 as DOI: 10.1124/dmd.116.069344
This article has not been copyedited and formatted. The final version may differ from this version.

Jose, CA) was used for statistical testing and graphing. Differences at α=0.05 were included because significance could not be ruled out. However, considering the multiple hypotheses tested, those comparisons with an α ≤ 0.01 were deemed most reliable. Fold differences in modified or variant histone chromatin occupancy between fetal and postnatal chromatin pools were calculated from the base two antilogarithm of the difference between the fetal and postnatal median ΔC_q values ($2^{\Delta Cq(postnatal) - \Delta Cq (fetal)}$). For ratio calculations, the log base two antilogarithm transformed negative ΔC_q values ($2^{-\Delta Cq}$) of chromatin occupancy by modified histones were calculated, and then the median occupancy values were divided to calculate the H3Ac/H3K27me3 and H3K4me3/H3K27me3 ratios.

Because chromatin occupancy by modified and variant histones for the majority of *CYP3A4* and *3A7* regulatory regions was significantly greater in fetal relative to postnatal chromatin, the relative nucleosome density was investigated using ChIP targeting histone H3. Chromatin occupancy by histone H3 was discovered to be a relatively constant difference between fetal and postnatal hepatocytes across all regulatory regions investigated, with occupancy about 30-fold greater in fetal hepatocytes (data not shown). To determine if the differential nucleosome density was exclusive to the major *CYP3A4* and *3A7* regulatory regions, the *CYP2C19* promoter nucleosome density was determined as above. CYP2C19, in contrast to CYP3A4 and 3A7, has a nearly constant expression level during hepatic development (Koukouritaki *et al.*, 2004). The difference in chromatin occupancy by H3 between fetal and postnatal chromatin on the *CYP2C19* promoter was similar to that observed for *CYP3A4* and *3A7* (data not shown). Thus, differential nucleosome density in fetal and postnatal chromatin was not considered for ΔC_q calculations as it represented a constant difference among all three genes investigated.

DMD Fast Forward. Published on February 26, 2016 as DOI: 10.1124/dmd.116.069344
This article has not been copyedited and formatted. The final version may differ from this version.

Results

The *CYP3A4* and *3A7* regulatory regions targeted in the current study, along with the known transcription factor binding sites within those regions, are depicted in Figure 1A and 1B, respectively. As an example of the assessments performed on each regulatory element, relative chromatin occupancy by modified histones and the transcription factor, C/EBPβ, within the CYP3A4 C/EBPβ element is shown in Figure 2. Occupancy by C/EBPβ served as a positive control for the ChIP analyses within this regulatory domain. Median ΔC_q values ± range are shown for C/EBPβ and H3K27me3. The ΔC_q value is inversely related to occupancy (*i.e.*, a lower ΔC_q indicates greater chromatin occupancy). Significantly greater H3K27me3 occupancy was observed in fetal relative to postnatal chromatin within all amplicons (1.6- to 14.9-fold, $p < 0.001$) and greater C/EBPβ occupancy was observed in fetal relative to the postnatal chromatin within amplicons 1 and 2 (2.5-fold, p=0.04 in amplicon 2 and 3.0-fold, p=0.02 in amplicon 1). No significant occupancy differences were observed in the remainder of the amplicons evaluated. Similar analyses were done for all *CYP3A4* and *3A7* elements. To facilitate visualization and evaluation, the data are depicted as heat maps, showing grouped median ΔCq values for fetal and postnatal primary hepatocyte chromatin (Figure 3 and 5) or the resulting p-values from the statistical comparison of fetal versus postnatal chromatin occupancy (Figure 4 and 6).

Modified and Variant Histone Occupancy of the *CYP3A4* Promoter in Fetal and Postnatal Hepatic Chromatin: In general, occupancy by modified and variant histones within the targeted *CYP3A4* regulatory domains (Figure 3A) was consistent with bivalent chromatin in the proximal promoter (*i.e.*, chromatin simultaneously occupied by H3K4me3 and H3K27me3) and poised enhancers (*i.e.* chromatin simultaneously occupied by H3K9me3, H3K27me3, and H3K4me1) for both postnatal and fetal chromatin (Figure 3B and 3C). Chromatin occupancy within the major regulatory regions by the relevant transcription factors was observed, indicating the detection of the expected regulatory region and also consistent with the overall poised state of

DMD Fast Forward. Published on February 26, 2016 as DOI: 10.1124/dmd.116.069344
This article has not been copyedited and formatted. The final version may differ from this version.

the *CYP3A4* promoter in both the fetus and postnatal hepatocytes. The proximal *CYP3A4* promoter in fetal chromatin exhibited greater occupancy by H4Ac, H2A.Z, and H3K27me3 in all amplicons relative to other modified histones evaluated, whereas high chromatin occupancy by H3K4me3 and H3K9me1 was restricted to the most proximal amplicon. Similar to the fetus, the *CYP3A4* proximal promoter in the postnatal hepatocytes also exhibited pronounced enrichment of H4Ac, H2A.Z, and H3K27me3 but also showed greater levels of H3K4me3 occupancy in all amplicons versus other modified histones (Figure 3C). In both postnatal and fetal chromatin, a marked chromatin occupancy difference was observed for amplicon 4 within the XREM region, having high occupancy by modified histones in striking contrast to the other amplicons within the region.

Differential *CYP3A4* Promoter Chromatin Occupancy in Fetal and Postnatal Hepatic Chromatin: Within *CYP3A4* proximal promoter amplicon 2, chromatin occupancy by H3K27me3 was greater in fetal compared to postnatal chromatin (13.0-fold, $p<0.001$, Mann-Whitney U test); similar but smaller differences were observed within amplicons 3 and 4 (2-fold, $p = 0.04$ and 9.2-fold, $p=0.03$, respectively, Mann-Whitney U test) (Figure 4). Occupancy by H3K9me3 was greater in fetal chromatin for amplicon 1 (2.8-fold, $p=0.003$, Mann-Whitney U test). However, similar to the modified histones associated with repression, H3K9me1 (3.7- to 7.5-fold, $p<0.001$ for all amplicons, Mann-Whitney U test) and H4Ac (5.3- to 7.0-fold $p<0.001$ for all amplicons, Mann-Whitney U test) chromatin occupancy also was greater in fetal relative to postnatal chromatin, as was occupancy by the variant histone, H2A.Z within two of four amplicons (4-fold, $p<0.001$ for amplicon 2, and 2.6-fold, $p=0.01$ for amplicon 3, Mann-Whitney U test). Chromatin occupancy by H3K4me3, generally associated with poised or active transcription, was greater in postnatal chromatin compared to the fetus for three of the four proximal promoter amplicons (1.5- and 2.8-fold, $p<0.001$ for amplicons 4 and 3, respectively, and 2.6-fold, $p=0.01$ for amplicon 1, Mann-Whitney U test) (Figure 4). Eight-fold greater occupancy by the transcription factor II D (TFIID) was seen in postnatal chromatin relative to the

DMD Fast Forward. Published on February 26, 2016 as DOI: 10.1124/dmd.116.069344
This article has not been copyedited and formatted. The final version may differ from this version.

fetus in amplicon 1 (p<0.001, Mann-Whitney U test), whereas in amplicon 2, fetal chromatin had a significantly greater occupancy (2.5-fold, p=0.005, Mann-Whitney U test) (Figure 4). Both amplicons cover the area containing the TATA box. Within the *CYP3A4* proximal promoter, the differences in chromatin occupancy by modified and variant histones was consistent with a more poised chromatin state in the fetal liver versus an active state in the postnatal liver.

The *CYP3A4* C/EBPβ regulatory domain exhibited greater chromatin occupancy by H3K27me3 (4.6- to 14.9-fold, p<0.001 for all amplicons, Mann-Whitney U test) and H3K9me3 (5.3-fold, p=0.03 for amplicon 1; 5.7-fold, p=0.004 for amplicon 2; 59.7-fold, p<0.001 for amplicon 4; 22.6-fold for amplicon 5, p<0.001; and 8.6-fold, p=0.002 for amplicon 6; Mann-Whitney U test) in fetal relative to postnatal chromatin (Figure 4). However, two amplicons exhibited greater occupancy by H4 acetylation in fetal compared to postnatal chromatin (5.7- and 8.0-fold for amplicons 4 and 5, respectively; p≤0.001, Mann-Whitney U test), and H3 acetylation was greater in the fetus across the majority of the region (16-fold, p=0.002 for amplicon 4; 6.1-fold, p=0.003 for amplicon 1; 5.3-fold p=0.02 and p=0.039 for amplicons 5 and 6, Mann-Whitney U test). Chromatin occupancy by variant histone H2A.Z also was greater in fetal chromatin across the majority of the region (1.9- to 16.0-fold, p<0.001 for amplicons 2, 4, and 5; 2.3-fold p=0.009 for amplicon 1, Mann-Whitney U test) (Figure 4). Overall, this chromatin occupancy by modified and variant histones yielded the impression that the C/EBPβ region was more repressed, but tending toward poised in the fetal versus postnatal liver.

Within all XREM amplicons, other than amplicon 4, fetal chromatin demonstrated greater occupancy relative to the postnatal chromatin by the two repressive modified histones, H3K27me3 (4.6- to 7.0-fold, p<0.001 for amplicons 1, 2, and 3; 6.5-fold p=0.005 for amplicon 5, Mann-Whitney U test) and H3K9me3 (10.6- to 22.6-fold, p<0.001 for amplicons 1, 2, 3, and 5, Mann-Whitney U test) (Figure 4). These repressive modified histones were present in conjunction with greater H3 and H4 acetylation in the fetal relative to postnatal hepatocytes within all amplicons, except amplicon 4 (H3Ac: 6.7-fold, p=0.002 for amplicon 2; 2.6 to 10.6-fold,

p<0.001 for amplicons 1, 3, and 5; H4Ac: 1.9-fold, p<0.015 for amplicon 1; 7.5 to 10.6-fold, p<0.001 for amplicons 2, 3, and 5, Mann-Whitney U test). In contrast to the majority of the regions within the XREM domain, amplicon 4, which covers two pregnane X receptor binding sites (Figure 1A), had significantly greater chromatin occupancy in postnatal compared to fetal chromatin by all of the modified histones associated with active transcription (Figure 4). The difference in occupancy by modified histones was consistent with the XREM domain being more poised in the fetal liver versus potentially active in the postnatal liver.

Within the *CYP3A4* CLEM4 domain, transcriptionally repressive H3K27me3 exhibited greater occupancy in fetal compared to postnatal chromatin in three of the four amplicons evaluated (5.3- to 13.0-fold, p<0.001 for amplicons 3, 7, and 8; 1.7-fold, p=0.002 for amplicon 5, Mann-Whitney U test). Similarly, transcriptionally repressive H3K9me3 also exhibited greater occupancy in fetal relative to postnatal chromatin (4.3-fold, p=0.004 for amplicon 8; 2.6- and 6.5-fold, p=0.02 for amplicon 3 and 7, respectively; 10.6-fold, p<0.001 for amplicon 5, Mann-Whitney U test) (Figure 4). However, in the amplicon containing the largest number of transcription factor binding sites (amplicon 5) (Figure 3A), chromatin occupancy by modified histones associated with active transcription was significantly greater in fetal versus postnatal chromatin (*e.g.*, H3Ac, 3.5-fold, p<0.001; and H3K4me1, 2.5-fold, p=0.01, Mann-Whitney U test) (Figure 4). In contrast, any differences in occupancy within CLEM4 element amplicon 5 by transcription factor USF1 (upstream stimulatory factor 1) in postnatal versus fetal hepatic chromatin was equivocal, despite this amplicon covering three USF1 binding sites (Figure 4). Overall, the differences in chromatin occupancy by modified histones within this region were consistent with a more poised enhancer in the fetal liver.

Evaluation of *CYP3A4* Regulatory Domain Chromatin Occupancy Using Modified Histone Ratios: The H3K4me3 to H3K27me3 ratio was previously investigated in chromatin regions surrounding the TSS of several promoters and exhibited a positive relationship to transcriptional activity (Roh *et al.*, 2006; De Gobbi *et al.*, 2011). Overall, the H3K4me3 to H3K27me3 ratio

within the *CYP3A4* proximal promoter was six-fold greater in postnatal versus fetal chromatin (Table 3). The highest postnatal value was observed in amplicon 2, which spans the TSS. The H3K4me3/H3K27me3 ratios were consistent with a chromatin structure supporting a more active transcriptional state in postnatal relative to fetal chromatin.

The H3Ac to H3K27me3 ratio was calculated for the *CYP3A4* enhancers. Active enhancers are enriched with H3K27ac whereas poised enhancers are enriched with H3K27me3 (Rada-Iglesias *et al.*, 2011; Creyghton *et al.*, 2010; Zentner *et al.*, 2011). Given that the H3Ac antibody used for ChIP has some specificity for H3K27ac (manufacturer data sheet), chromatin occupancy by H3Ac was used as a general proxy for H3K27ac occupancy. The H3Ac to H3K27me3 ratios for the CLEM4 and C/EBPβ binding regions were approximately 2-fold greater in postnatal versus fetal chromatin (Table 4). Overall, the ratio within the XREM region was similar for postnatal and fetal chromatin, but within amplicon 4, which covers two PXR binding sites, the postnatal ratio was 4-fold greater than the fetal ratio. Overall, the ratios in the XREM domain had values less than one, indicating a greater presence of H3K27me3, but suggested a more active enhancer state in the postnatal liver relative to the fetus for the CLEM4 and C/EBPβ domains and amplicon 4 within the XREM region.

Modified and Variant Histone Occupancy of the *CYP3A7* Promoter in Fetal and Postnatal Hepatic Chromatin: Occupancy of the major *CYP3A7* regulatory domains (Figure 5A) by transcription factors with known binding sites in each domain was evaluated both as a control and to assess overall DNA access. Moderate occupancy of the proximal promoter and C/EBPβ regulatory domain was observed with TFIID and C/EBPβ, respectively, in fetal chromatin, but little or no HNF4α occupancy was observed in the XREM domain (Figure 5B). In contrast, only C/EBPβ and HNF4α occupancy was observed in postnatal chromatin (Figure 5C).

Modified and variant histone occupancy within the targeted *CYP3A7* promoter domains (Figure 5A) in general was consistent with bivalent chromatin. For the *CYP3A7* proximal promoter, modest but near equal occupancy of H3K4me3, H3K27me3 and H2A.Z. was

DMD Fast Forward. Published on February 26, 2016 as DOI: 10.1124/dmd.116.069344
This article has not been copyedited and formatted. The final version may differ from this version.

observed in both fetal (Figure 5B) and postnatal (Figure 5C) chromatin. The proximal promoter and C/EBPβ regulatory domain in the fetal chromatin exhibited greater occupancy by H2A.Z in two-thirds and three-quarters of the amplicons, respectively, relative to occupancy within the other amplicons (Figure 5B). Additionally, occupancy within the *CYP3A7* XREM and C/EBPβ domains was consistent with poised enhancers, exhibiting occupancy by H3K27me3, H3K9me3, and H3K4me1 (Figure 5B). In the postnatal hepatocyte (Figure 5C), assessment of occupancy by modified histones was consistent with bivalent chromatin being present in the proximal promoter whereas the other major *CYP3A7* regulatory regions exhibited the lowest occupancy ranges ($\Delta C_q > 11$) by most of the modified histones evaluated; if anything, these domains appeared to be dominated by modified histones associated with active or poised transcriptional states. Occupancy by H4Ac was greatest in two-thirds of the amplicons within the proximal promoter and half of the amplicons within the C/EBPβ binding region. Relative occupancy by H2A.Z also was greatest in two-thirds of the amplicons within the proximal promoter. Overall, the occupancy by modified and variant histones did not appear consistent with the high *CYP3A7* expression observed in fetal liver (Stevens *et al.*, 2003).

Differential *CYP3A7* Promoter Chromatin Occupancy in Fetal and Postnatal Hepatic Chromatin: Occupancy differences between fetal and postnatal chromatin were minimal in the *CYP3A7* proximal promoter (Figure 6). Proximal promoter occupancy by the repressive modified histones, H3K27me3 and H3K9me3 was greater in fetal chromatin. For H3K27me3, this was true for all amplicons tested (4.0- to 12.1-fold, $p<0.001$, Mann-Whitney U test) while for H3K9me3, occupancy was greater across two amplicons within the proximal promoter (3.0-fold, $p\leq0.001$ for amplicon N; 3.0-fold, $p=0.02$ for amplicon L, Mann-Whitney U test). TFIID occupancy was greater (3.0-fold, $p=0.002$, Mann-Whitney U test) in postnatal chromatin relative to that of the fetus for amplicon M, which covers the TATA box. Greater occupancy within this same amplicon was observed for H3K4me3 and H3Ac, both associated with chromatin structure favoring active transcriptional states. The occupancy by modified histones and transcription

factors within the proximal promoter appeared to be consistent with a repressed transcriptional state in the fetal relative to the postnatal hepatocyte, opposite to what might be expected based on known expression patterns (Stevens *et al.*, 2003).

Within the *CYP3A7* C/EBPβ regulatory domain, differential chromatin occupancy by modified and variant histones was similar to that observed for the *CYP3A4* C/EBPβ domain with the exception of H3K9me3, which exhibited greater occupancy in fetal relative to postnatal chromatin on the periphery of the targeted region (3.2-fold, $p=0.04$ for amplicon J; 17.1-fold, $p<0.001$ for amplicon F, Mann-Whitney U test) (Figure 6). Chromatin occupancy by both H3K27me3 and H2A.Z was greater (H3K27me3, 8.0- to 19.7-fold, $p\leq0.001$ for all amplicons, and H2A.Z, 2.3-fold, $p=0.01$ for amplicon G; 3.5- to 5.7-fold, $p<0.001$ for amplicons F, I, and J, Mann-Whitney U test) in fetal hepatic chromatin across the region relative to postnatal chromatin. More consistent with the known CYP3A7 developmental expression pattern (Stevens *et al*., 2003), chromatin occupancy by modified histones associated with active transcription was greater in fetal compared to postnatal chromatin for some, but not all of the amplicons. Similar to the *CYP3A4* C/EBPβ binding region, chromatin occupancy by C/EBPβ was similar between postnatal and fetal chromatin (Figure 6). Overall, these data suggest the chromatin structure within the C/EBPβ domain is more poised in the fetal relative to the postnatal liver.

In the *CYP3A7* XREM region, chromatin occupancy by H3K27me3 and H3K9me3 was greater in fetal versus postnatal chromatin (H3K27me3, 9.8- to 29.9-fold, $p<0.001$ for all amplicons, and H3K9me3, 4.3-fold, $p=0.003$ for amplicon E; 4.6-fold, $p<0.001$ for amplicon C, Mann-Whitney U test) (Figure 6). Greater fetal chromatin occupancy by H3Ac and H4Ac also was observed in two of the three amplicons within this module (H3Ac, 3.7-fold, $p=0.02$; 3.7-fold, $p<0.001$ for amplicon C and E and H4Ac, 1.5-fold, $p=0.01$ for amplicon C; 1.7-fold, $p=0.004$ for amplicon E, Mann-Whitney U test). XREM occupancy by HNF4α in postnatal and fetal chromatin was equivalent (Figure 6). Differential chromatin occupancy by modified histones in the XREM was consistent with a more poised enhancer in fetal versus postnatal chromatin.

DMD Fast Forward. Published on February 26, 2016 as DOI: 10.1124/dmd.116.069344
This article has not been copyedited and formatted. The final version may differ from this version.

Evaluation of *CYP3A7* Regulatory Domain Chromatin Occupancy Using Modified Histone Ratios: The H3K4me3/H3K27me3 ratio within the *CYP3A7* proximal promoter was approximately 10-fold greater in postnatal chromatin compared to the fetus (Table 5). This difference is consistent with postnatal liver having greater transcriptional activity relative to fetal liver.

Within the *CYP3A7* enhancers, greater H3Ac/H3K27me3 values were observed in postnatal chromatin relative to the fetus. The XREM region and C/EBPβ binding regions had H3Ac/H3K27me3 values 10- and 4-fold greater, respectively, in postnatal relative to the fetal chromatin (Table 6). Further, the postnatal ratios for amplicons A and C within the XREM were greater than one, indicating a greater occupancy by H3Ac relative to H3K27me3. Similarly, H3Ac/H3K27me3 values within the C/EBPβ regulatory domain were greater than one in amplicons G and I. These ratios were consistent with a more active enhancer state within postnatal chromatin relative to the fetus and are inconsistent with the active enhancer state expected in the fetus based on temporal-specific CYP3A7 expression patterns.

Discussion

Despite the demonstrated clinical significance of age-dependent changes in hepatic CYP3A4 and 3A7 expression, little is known regarding the molecular mechanisms controlling the developmental expression of these two enzymes (reviewed in Hines 2008). The current study evaluated a possible role for epigenetic-mediated changes in chromatin structure regulating CYP3A4 and 3A7 ontogeny. Chromatin occupancy by seven modified and one variant histone was determined as indicators of chromatin structure within the major *CYP3A4* and *3A7* regulatory domains in human fetal and postnatal chromatin prepared from primary fetal and postnatal hepatocytes. These epigenetic changes were investigated at time points representing the CYP3A4 and 3A7 expression extremes during ontogeny, *i.e.*, early second trimester and greater than 1 year of age (Stevens *et al.*, 2003).

The major *CYP3A4* regulatory regions in fetal and postnatal chromatin were occupied by relatively high levels of both H3K4me3 and H3K27me3, which have been linked to chromatin structure associated with opposing transcriptional states. Concomitant occupancy with such oppositely acting, modified histones is typical of bivalent chromatin, *i.e.*, chromatin poised for active gene expression (Bernstein *et al.*, 2006). The H3K4me3/H3K27me3 ratio around the TSS exhibits a positive relationship with transcriptional activity (Roh *et al.*, 2006; De Gobbi *et al.*, 2011). In the current study, the average H3K4me3/H3K27me3 occupancy ratio in postnatal chromatin was greater than that observed in fetal chromatin, consistent with higher levels of CYP3A4 expression in postnatal liver.

Both postnatal and fetal chromatin exhibited relatively high H2A.Z occupancy within the *CYP3A4* proximal promoter, and compared to fetal chromatin, postnatal chromatin had significantly greater occupancy by H3K4me3 and TFIID within this domain. Occupancy by H2A.Z is associated with RNA polymerase II recruitment (Hardy *et al.*, 2009); TFIID binding initiates RNA polymerase II recruitment (Orphanides *et al.*, 1996) and H3K4me3 occupancy peaks around the TSS are associated with actively transcribed genes (Barski *et al*., 2007). Taken together, these observations are consistent with a more permissive chromatin structure in the postnatal versus fetal liver.

Chromatin occupancy by modified and variant histones observed within the *CYP3A4* CLEM4, XREM, and C/EBPβ regulatory domains were indicative of less transcription in the fetal relative to the postnatal liver. Occupancy by H3K27me3, H3K9me3, and H3K4me1 was significantly greater in fetal relative to postnatal chromatin across all three of these regions. Taken together, these results support poised *CYP3A4* enhancers in the fetal liver, which are associated with lower gene expression relative to active enhancers (Rada-Iglesias *et al.*, 2011; Zentner *et al.*, 2011). Greater occupancy by H3K4me1 and H3Ac, both associated with active transcriptional states, was observed in postnatal relative to fetal chromatin for one amplicon probe within the XREM region. This observation was peculiar because the region was flanked

by significantly greater occupancy by modified histones associated with poised transcriptional state in fetal relative to postnatal chromatin. However, this finding may be explained by high HNF4α occupancy within this same domain postnatally, which can promote histone acetylation (Soutoglou *et al.*, 2001). Additionally, the greater H3Ac/H3K27me3 ratios in postnatal chromatin relative to fetus for the CLEM4, C/EBPβ, and XREM binding region indicated a more active enhancer state in the postnatal liver. Overall, the chromatin occupancy by modified and variant histones and transcription factors within known *CYP3A4* regulatory elements was consistent with epigenetic-mediated changes in chromatin structure serving as an important mechanism regulating CYP3A4 ontogeny.

A less convincing occupancy pattern was observed to support chromatin structural changes regulating CYP3A7 ontogeny. The average H3K4me3/H3K27me3 ratio (Roh *et al.*, 2006; De Gobbi *et al.*, 2011) within the proximal promoter of postnatal hepatic chromatin was greater than the fetal hepatic chromatin ratio, consistent with greater *CYP3A7* transcription in postnatal relative to fetal liver. Further, greater occupancy by TFIID, H3K4me3 and H3Ac, all associated with a transcriptionally active promoter *(*Barski *et al.*, 2007; Wang *et al.*, 2008; Kim *et al.*, 2005), was observed in postnatal relative to fetal chromatin. Similarly, occupancy patterns by modified and variant histones in the *CYP3A7* XREM and C/EBPβ domains were consistent with more active enhancer activity in postnatal versus fetal liver. Although the greater occupancy by H2A.Z in fetal compared to postnatal chromatin is consistent with a more accessible enhancer (Jin and Felsenfeld, 2007; Calo and Wysocka, 2013), the significantly greater occupancy by H3K27me3 in fetal relative to postnatal hepatic chromatin across both regions, was more suggestive of poised enhancers. Several amplicon probes showed greater H3Ac fetal chromatin occupancy relative to postnatal chromatin, but the H3Ac/H3K27me3 ratio within these regions was lower in fetal relative to postnatal chromatin, again indicating a more poised chromatin state in fetal chromatin. Overall, the chromatin occupancy pattern by modified histones within the *CYP3A7* enhancer and promoter regions is inconsistent with known CYP3A7

DMD Fast Forward. Published on February 26, 2016 as DOI: 10.1124/dmd.116.069344
This article has not been copyedited and formatted. The final version may differ from this version.

developmental expression and would not support epigenetic-mediated changes in chromatin structure being a major mechanism regulating CYP3A7 ontogeny.

Dynamic chromatin occupancy by modified histones is associated with mouse hepatic Cyp3a age-dependent expression changes that somewhat resemble human CYP3A ontogeny (Li *et al.*, 2009). Cyp3a16 and Cyp3a11 mRNA ontogeny resembles CYP3A7 and 3A4 ontogeny, respectively (Hart *et al.*, 2009). The human H3K27me3 occupancy pattern observed in the current study contrasts with both of the patterns previously observed for mouse *Cyp3a16* and *Cyp3a11* (Li *et al.*, 2009). However, the observed occupancy pattern for H3K4me2, which has a functional role similar to H3K4me3 (Barski *et al.*, 2007), is consistent with the observed H3K4me3 chromatin occupancy pattern observed for the *CYP3A4* proximal promoter in the current study. Thus, epigenetic-mediated changes in chromatin structure appear to be a mechanism regulating CYP3A ontogeny in both the mouse and human.

CYP3A genetic variation might confound the interpretation of the modified and variant histone occupancy data if alleles were present in the chromatin pools that substantially impacted expression. More than forty *CYP3A4* allelic variants have been reported (http://www.cypalleles.ki.se/cyp3a4.htm); however, these variants exhibit limited effects on expression and/or exhibit a low prevalence. Among the six reported *CYP3A7* alleles (Sim *et al.*, 2005; Rodriguez-Antona *et al.*, 2005; Kuehl *et al.*, 2001), *CYP3A7*1C* is associated with adult hepatic CYP3A7 expression (Burk *et al.*, 2002; Sim *et al.*, 2005). However, this allele was not present in either the postnatal or fetal chromatin pools used in the current study based on an assessment by DNA sequencing (data not shown). Thus, neither the observed patterns of chromatin occupancy by histones nor their interpretation were likely affected by genetic variation at these loci.

Differential transcription factor expression and/or binding might also contribute to regulating differential CYP3A expression trajectories during hepatic development. As a possible example, C/EBPβ plays a major role in stem cell differentiation into a mature hepatocyte

phenotype and plays a major in role in regulating CYP3A expression through the C/EBPβ regulatory domain (Figure 1). Thus, enhanced C/EBPβ expression has been associated with relatively higher *CYP3A4* expression levels (Talens-Visconti *et al.*, 2006). However, three C/EBPβ isoforms exist that exhibit distinct functional differences and age-dependent expression patterns (Saint-Auret *et al.*, 2011). These three isoforms could not be discerned in the current study because the antibody used for C/EBPβ immunoprecipitation does not discriminate between them. Thus, changes in the relative expression levels of C/EBPβ isoforms as a function of age may contribute to regulating *CYP3A4* chromatin remodeling during hepatic development and CYP3A4 ontogeny.

A limitation of the current study is the heterogeneous cell composition of the fetal liver samples used to prepare chromatin. This problem was hard to overcome because of the difficulty in obtaining fetal primary hepatocytes combined with the number of cells needed to prepare sufficient chromatin for ChIP experiments. The fetal hepatic chromatin pool was prepared from second trimester fetal livers that contain a heterogeneous mixture of hepatocytes, hepatocyte precursors, hematopoietic stem cells, and mesenchymal cells (Gridelli *et al.*, 2012; Nava *et al*., 2005; Mahieu-Caputo *et al.*, 2004), several of which exhibit low and undetectable CYP3A4 and 3A7 mRNA expression, respectively (Shao *et al*., 2007). This fetal hepatocyte dilution likely would increase the observed occupancy by modified histones associated with repressed transcription and result in an observed occupancy pattern inconsistent with known CYP3A7 ontogeny. In contrast, given the low to absent CYP3A4 expression during this same gestational period, there would be little or no impact of fetal hepatocyte dilution on the interpretation of the CYP3A4 chromatin occupancy data. Thus, the likely heterogeneous fetal liver cell population used to derive chromatin is a possible design limitation and may have impacted the interpretation of fetal, but not postnatal hepatic chromatin structural dynamics.

The current study has, for the first time, determined fetal and postnatal chromatin occupancy by modified and variant histones for the major *CYP3A4* and *3A7* regulatory domains and evaluated these epigenetic changes relative to known CYP3A4 and 3A7 ontogeny. Occupancy by modified histones was consistent with chromatin structural changes contributing to the mechanisms regulating *CYP3A4* ontogeny. The data were less conclusive regarding *CYP3A7*, which may have been caused by heterogeneity in the fetal, but not postnatal cell preparations used to prepare chromatin. Additionally, mechanisms other than histone modification, such as differential DNA methylation or differential miRNA expression may have a more important role in regulating *CYP3A7* ontogeny.

DMD Fast Forward. Published on February 26, 2016 as DOI: 10.1124/dmd.116.069344
This article has not been copyedited and formatted. The final version may differ from this version.

Authorship Contributions

Participated in research design: Giebel, Shadley, Dorko, Gramignoli, Strom, Hines

Conducted experiments: Giebel, Shadley

Contributed tissue samples: Strom, Dorko, Gramignoli

Contributed statistical analysis support: Yan, Simpson,

Performed data analysis: Giebel, Shadley, Yan, Simpson, McCarver, Hines

Wrote or contributed to the writing of the manuscript: Giebel, McCarver, Hines

References

Alcorn J and McNamara P J (2008) Using Ontogeny Information to Build Predictive Models for Drug Elimination. *Drug Discov Today* 13:507-512.

Barski A, Cuddapah S, Cui K, Roh T Y, Schones D E, Wang Z, Wei G, Chepelev I and Zhao K (2007) High-Resolution Profiling of Histone Methylations in the Human Genome. *Cell* 129:823-837.

Bernstein BE, Mikkelsen T S, Xie X, Kamal M, Huebert D J, Cuff J, Fry B, Meissner A, Wernig M, Plath K, Jaenisch R, Wagschal A, Feil R, Schreiber S L and Lander E S (2006) A Bivalent Chromatin Structure Marks Key Developmental Genes in Embryonic Stem Cells. *Cell* 125:315-326.

Burk O, Tegude H, Koch I, Hustert E, Wolbold R, Glaeser H, Klein K, Fromm M F, Nuessler A K, Neuhaus P, Zanger U M, Eichelbaum M and Wojnowski L (2002) Molecular Mechanisms of Polymorphic CYP3A7 Expression in Adult Human Liver and Intestine. *J Biol Chem* 277:24280-24288.

Burns MJ, Nixon G J, Foy C A and Harris N (2005) Standardisation of Data From Real-Time Quantitative PCR Methods - Evaluation of Outliers and Comparison of Calibration Curves. *BMC Biotechnol* 5:31.

Calo E and Wysocka J (2013) Modification of Enhancer Chromatin: What, How, and Why? *Mol Cell* 49:825-837.

Cereghini S (1996) Liver-Enriched Transcription Factors and Hepatocyte Differentiation. *FASEB J* 10:267-282.

Creyghton MP, Cheng A W, Welstead G G, Kooistra T, Carey B W, Steine E J, Hanna J, Lodato M A, Frampton G M, Sharp P A, Boyer L A, Young R A and Jaenisch R (2010) Histone H3K27ac Separates Active From Poised Enhancers and Predicts Developmental State. *Proc Natl Acad Sci U S A* 107:21931-21936.

De Gobbi M, Garrick D, Lynch M, Vernimmen D, Hughes J R, Goardon N, Luc S, Lower K M, Sloane-Stanley J A, Pina C, Soneji S, Renella R, Enver T, Taylor S, Jacobsen S E, Vyas P, Gibbons R J and Higgs D R (2011) Generation of Bivalent Chromatin Domains During Cell Fate Decisions. *Epigenetics Chromatin* 4:9.

de Wildt SN, Kearns G L, Leeder J S and van den Anker J N (1999) Cytochrome P450 3A: Ontogeny and Drug Disposition. *Clin Pharmacokinet* 37:485-505.

Gramignoli R, Green ML, Than V, Dorko K, Skvorak KJ, Marongiu F, Zao W, Venkataramanan R, Ellis ECS, Geller D, Breite AG, Dwulet FE, McCarthy RC and Strom SC (2012) Development and application of purified tissue dissociation enzyme mixtures for human hepatocyte isolation. *Cell Transplant* 21:1245-1260.

Gramignoli R, Tahan V, Dorko K, Venkataramanan R, Fox IJ, Ellis, ECS, Vosough M and Strom SC (2014) Rapid and Sensitive Assessment of Human Hepatocyte Functions. *Cell Transplant* 23:1545-1556.

Gridelli B, Vizzini G, Pietrosi G, Luca A, Spada M, Gruttadauria S, Cintorino D, Amico G, Chinnici C, Miki T, Schmelzer E, Conaldi P G, Triolo F and Gerlach J C (2012) Efficient Human Fetal Liver Cell Isolation Protocol Based on Vascular Perfusion for Liver Cell-Based Therapy and Case Report on Cell Transplantation. *Liver Transpl* 18:226-237.

Hardy S, Jacques P E, Gevry N, Forest A, Fortin M E, Laflamme L, Gaudreau L and Robert F (2009) The Euchromatic and Heterochromatic Landscapes Are Shaped by Antagonizing Effects of Transcription on H2A.Z Deposition. *PLoS Genet* 5:e1000687.

Hart SN, Cui Y, Klaassen C D and Zhong X B (2009) Three Patterns of Cytochrome P450 Gene Expression During Liver Maturation in Mice. *Drug Metab Dispos* 37:116-121.

Hines RN (2008) The Ontogeny of Drug Metabolism Enzymes and Implications for Adverse Drug Events. *Pharmacol Ther* 118:250-267.

Jin C and Felsenfeld G (2007) Nucleosome Stability Mediated by Histone Variants H3.3 and H2A.Z. *Genes Dev* 21:1519-1529.

Kiefer JC (2007) Epigenetics in Development. *Dev Dyn* 236:1144-1156.

Kim DH, Behlke M A, Rose S D, Chang M S, Choi S and Rossi J J (2005) Synthetic DsRNA Dicer Substrates Enhance RNAi Potency and Efficacy. *Nat Biotechnol* 23:222-226.

Klein K, Thomas M, Winter S, Nussler A K, Niemi M, Schwab M and Zanger U M (2012) PPARA: a Novel Genetic Determinant of CYP3A4 in Vitro and in Vivo. *Clin Pharmacol Ther* 91:1044-1052.

Koukouritaki SB, Manro J R, Marsh S A, Stevens J C, Rettie A E, McCarver D G and Hines R N (2004) Developmental Expression of Human Hepatic CYP2C9 and CYP2C19. *J Pharmacol Exp Ther* 308:965-974.

Kuehl P, Zhang J, Lin Y, Lamba J, Assem M, Schuetz J, Watkins P B, Daly A, Wrighton S A, Hall S D, Maurel P, Relling M, Brimer C, Yasuda K, Venkataramanan R, Strom S, Thummel K, Boguski M S and Schuetz E (2001) Sequence Diversity in CYP3A Promoters and Characterization of the Genetic Basis of Polymorphic CYP3A5 Expression. *Nat Genet* 27:383-391.

Li Y, Cui Y, Hart S N, Klaassen C D and Zhong X B (2009) Dynamic Patterns of Histone Methylation Are Associated With Ontogenic Expression of the Cyp3a Genes During Mouse Liver Maturation. *Mol Pharmacol* 75:1171-1179.

Mahieu-Caputo D, Allain J E, Branger J, Coulomb A, Delgado J P, Andreoletti M, Mainot S, Frydman R, Leboulch P, Di Santo J P, Capron F and Weber A (2004) Repopulation of Athymic Mouse Liver by Cryopreserved Early Human Fetal Hepatoblasts. *Hum Gene Ther* 15:1219-1228.

Martignoni M, Groothuis G M and de K R (2006) Species Differences Between Mouse, Rat, Dog, Monkey and Human CYP-Mediated Drug Metabolism, Inhibition and Induction. *Expert Opin Drug Metab Toxicol* 2:875-894.

Matsumura K, Saito T, Takahashi Y, Ozeki T, Kiyotani K, Fujieda M, Yamazaki H, Kunitoh H and Kamataki T (2004) Identification of a Novel Polymorphic Enhancer of the Human CYP3A4 Gene. *Mol Pharmacol* 65:326-334.

Nava S, Westgren M, Jaksch M, Tibell A, Broome U, Ericzon B G and Sumitran-Holgersson S (2005) Characterization of Cells in the Developing Human Liver. *Differentiation* 73:249-260.

Orphanides G, Lagrange T and Reinberg D (1996) The General Transcription Factors of RNA Polymerase II. *Genes Dev* 10:2657-2683.

Ourlin JC, Jounaidi Y, Maurel P and Vilarem M J (1997) Role of the Liver-Enriched Transcription Factors C/EBP Alpha and DBP in the Expression of Human CYP3A4 and CYP3A7. *J Hepatol* 26 Suppl 2:54-62.

Perera MA, Thirumaran R K, Cox N J, Hanauer S, Das S, Brimer-Cline C, Lamba V, Schuetz E G, Ratain M J and Di R A (2009) Prediction of CYP3A4 Enzyme Activity Using Haplotype Tag SNPs in African Americans. *Pharmacogenomics J* 9:49-60.

Plant N (2007) The Human Cytochrome P450 Sub-Family: Transcriptional Regulation, Inter-Individual Variation and Interaction Networks. *Biochim Biophys Acta* 1770:478-488.

Rada-Iglesias A, Bajpai R, Swigut T, Brugmann S A, Flynn R A and Wysocka J (2011) A Unique Chromatin Signature Uncovers Early Developmental Enhancers in Humans. *Nature* 470:279-283.

Riffel AK, Schuenemann E and Vyhlidal C A (2009) Regulation of the CYP3A4 and CYP3A7 Promoters by Members of the Nuclear Factor I Transcription Factor Family. *Mol Pharmacol* 76:1104-1114.

Rodriguez-Antona C, Axelson M, Otter C, Rane A and Ingelman-Sundberg M (2005) A Novel Polymorphic Cytochrome P450 Formed by Splicing of CYP3A7 and the Pseudogene CYP3AP1. *J Biol Chem* 280:28324-28331.

Roh TY, Cuddapah S, Cui K and Zhao K (2006) The Genomic Landscape of Histone Modifications in Human T Cells. *Proc Natl Acad Sci U S A* 103:15782-15787.

Saint-Auret G, Danan J L, Hiron M, Blache C, Sulpice E, Tendil S, Daveau M, Gidrol X and Salier J P (2011) Characterization of the Transcriptional Signature of C/EBPbeta Isoforms (LAP/LIP) in Hep3B Cells: Implication of LIP in Pro-Survival Functions. *J Hepatol* 54:1185-1194.

Saito T, Takahashi Y, Hashimoto H and Kamataki T (2001) Novel Transcriptional Regulation of the Human CYP3A7 Gene by Sp1 and Sp3 Through Nuclear Factor Kappa B-Like Element. *J Biol Chem* 276:38010-38022.

Schuetz EG (2004) Lessons From the CYP3A4 Promoter. *Mol Pharmacol* 65:279-281.

Shao J, Stapleton P L, Lin Y S and Gallagher E P (2007) Cytochrome P450 and Glutathione S-Transferase MRNA Expression in Human Fetal Liver Hematopoietic Stem Cells. *Drug Metab Dispos* 35:168-175.

Sharma S, Ellis E C, Gramignoli R, Dorko K, Tahan V, Hansel M, Mattison D R, Caritis S N, Hines R N, Venkataramanan R and Strom S C (2013) Hepatobiliary Disposition of 17-OHPC and Taurocholate in Fetal Human Hepatocytes: a Comparison With Adult Human Hepatocytes. *Drug Metab Dispos* 41:296-304.

Sim SC, Edwards R J, Boobis A R and Ingelman-Sundberg M (2005) CYP3A7 Protein Expression Is High in a Fraction of Adult Human Livers and Partially Associated With the *CYP3A7*1C* Allele. *Pharmacogenet Genomics* 15:625-631.

Soutoglou E, Viollet B, Vaxillaire M, Yaniv M, Pontoglio M and Talianidis I (2001) Transcription Factor-Dependent Regulation of CBP and P/CAF Histone Acetyltransferase Activity. *EMBO J* 20:1984-1992.

Stevens JC, Hines R N, Gu C, Koukouritaki S B, Manro J R, Tandler P J and Zaya M J (2003) Developmental Expression of the Major Human Hepatic CYP3A Enzymes. *J Pharmacol Exp Ther* 307:573-582.

Suganuma T and Workman J L (2011) Signals and Combinatorial Functions of Histone Modifications. *Annu Rev Biochem* 80:473-499.

Talens-Visconti R, Bonora A, Jover R, Mirabet V, Carbonell F, Castell J V and Gomez-Lechon M J (2006) Hepatogenic Differentiation of Human Mesenchymal Stem Cells From Adipose Tissue in Comparison With Bone Marrow Mesenchymal Stem Cells. *World J Gastroenterol* 12:5834-5845.

Wang Z, Zang C, Rosenfeld J A, Schones D E, Barski A, Cuddapah S, Cui K, Roh T Y, Peng W, Zhang M Q and Zhao K (2008) Combinatorial Patterns of Histone Acetylations and Methylations in the Human Genome. *Nat Genet* 40:897-903.

Williams JA, Hyland R, Jones B C, Smith D A, Hurst S, Goosen T C, Peterkin V, Koup J R and Ball S E (2004) Drug-Drug Interactions for UDP-Glucuronosyltransferase Substrates: a Pharmacokinetic Explanation for Typically Observed Low Exposure (AUCi/AUC) Ratios. *Drug Metab Dispos* 32:1201-1208.

Zentner GE, Tesar P J and Scacheri P C (2011) Epigenetic Signatures Distinguish Multiple Classes of Enhancers With Distinct Cellular Functions. *Genome Res* 21:1273-1283.

Zhou VW, Goren A and Bernstein B E (2011) Charting Histone Modifications and the Functional Organization of Mammalian Genomes. *Nat Rev Genet* 12:7-18.

Footnotes

This work was supported in part by the National Institutes of Health [Grant GM081344] (RNH, DGM) and the Swedish Research Council, Ventenskapprådet and the Torsten och Ragnar Söderberg Stiftelse (RG, SCS).

DMD Fast Forward. Published on February 26, 2016 as DOI: 10.1124/dmd.116.069344
This article has not been copyedited and formatted. The final version may differ from this version.

Figure Legends

Figure 1: (A) *CYP3A4* and (B) *CYP3A7* promoters and known regulatory regions. The major regulatory regions, the constitutive liver enhancer module 4 (CLEM4), xenobiotic response enhancer module (XREM), the CCAAT-enhancer binding protein beta binding region (C/EBPβ), and proximal promoter are expanded with transcription factor binding sites indicated (HNF4, hepatocyte nuclear factor 4; NF1/HNF3, nuclear factor 1/hepatocyte nuclear factor 3; KLF9, Kruppel-like factor 9; PXR, pregnane X receptor; PAR, proline acid rich factor; USF1, upstream factor 1; Sp/XKLF, sephacryl phosphocellulose/Kruppel-like factor; AP1, activator protein 1).

Figure 2: Chromatin occupancy by H3K27me3 and C/EBPβ within the *CYP3A4* C/EBPβ binding region in fetal (○) and postnatal (●) hepatic chromatin pools. The C/EBPβ binding region with targeted amplicons and transcription factor binding sites is indicated. Median ΔC_q values are shown plus the data range (* = p ≤0.05, *** = p ≤0.001, Mann-Whitney U test).

Figure 3: *CYP3A4* promoter occupancy by modified and variant histones or transcription factors. (A) Shown are the four known *CYP3A4* regulatory domains probed in the current study, all known transcription factors binding within each domain, and the qPCR amplicons used to evaluate ChIP enrichment. ChIP was performed with antibodies for modified and variant histones, as well as a single transcription factor known to bind within each domain, followed by qPCR to quantify occupancy. The data for pooled (B) fetal (N=14) and (C) postnatal (N=10) hepatic chromatin are shown as blue-tinted heat maps of the ΔC_q value median ranges of a minimum of three experiments for each amplicon within the indicated *CYP3A4* region (N/A = not assayed). Modified and variant histones are grouped into those associated with active (green font), poised (blue font), or inactive transcription (red font). The relevant occupancy by select transcription factors (black font) also is shown (HNF4, hepatocyte nuclear factor 4; NF1/HNF3, nuclear factor 1/hepatocyte nuclear factor 3; KLF9, Kruppel-like factor 9; PXR, pregnane X

receptor; PAR, proline acid rich factor; USF1, upstream factor 1; Sp/XKLF, sephacryl phosphocellulose/Kruppel-like factor; AP1, activator protein 1).

Figure 4: Differences in *CYP3A4* promoter occupancy by modified and variant histones between pooled fetal (N=14) and pooled postnatal (N=10) hepatic chromatin were evaluated using a Mann-Whitney U-test. The data are shown as red- or green-tinted heat maps (see legend) of the p-value ranges. Red and green tints indicate increasingly greater degrees of significant differences between chromatin occupancy between postnatal and fetal chromatin, respectively. Yellow indicates no significant difference (NS). N/A indicates not assayed. Modified and variant histones are grouped into those associated with active (green font), poised (blue font), or inactive transcription states (red font). The relevant occupancy by transcription factors (black font) also is shown.

Figure 5: *CYP3A7* promoter occupancy by modified and variant histones or transcription factors. (A) Shown are the three known *CYP3A7* regulatory domains probed in the current study, all known transcription factors binding within each domain, and the qPCR amplicons used to evaluate ChIP enrichment. ChIP was performed with antibodies for modified and variant histones, as well as a single transcription factor known to bind within each domain, followed by qPCR to quantify occupancy. The data for pooled (B) fetal (N=14) and (C) postnatal (N=10) hepatic chromatin are shown as blue-tinted heat maps of the ΔC_q value median ranges of a minimum of three experiments for each amplicon within the indicated *CYP3A7* region (N/A = not assayed). Modified and variant histones are grouped into those associated with active (green font), poised (blue font), or inactive transcription (red font). The relevant occupancy by select transcription factors (black font) also is shown (HNF4, hepatocyte nuclear factor 4; NF1/HNF3, nuclear factor 1/hepatocyte nuclear factor 3; KLF9, Kruppel-like factor 9; C/EBPβ, CCAAT Enhancer Binding Protein β; PXR, pregnane X receptor).

DMD Fast Forward. Published on February 26, 2016 as DOI: 10.1124/dmd.116.069344
This article has not been copyedited and formatted. The final version may differ from this version.

Figure 6: Differences in *CYP3A7* promoter occupancy by modified and variant histones or transcription factors between pooled fetal (N=14) and pooled postnatal (N=10) hepatic chromatin were evaluated using a Mann-Whitney U-test. The data are shown as red- or green-tinted heat maps (see legend) of the p-value ranges. Red and green tints indicate greater occupancy in the postnatal and fetal chromatin, respectively. Yellow indicates no significant difference (NS). N/A indicates not assayed. Modified and variant histones are grouped into those associated with active (green font), poised (blue font), or inactive transcription (red font). The relevant occupancy by transcription factors (black font) also is shown.

DMD Fast Forward. Published on February 26, 2016 as DOI: 10.1124/dmd.116.069344
This article has not been copyedited and formatted. The final version may differ from this version.

Table 1. Association of Modified and Variant Histone Chromatin Occupancy with Transcriptional States[a]

Transcriptional State	Domain	Modified or Variant Histone
Repressed	Proximal Promoter	H3K27me3 H3K9me3
Poised	Proximal Promoter	H3K4me3 H3K27me3 H2A.Z.
	Enhancer	H3K4me1 H3K27me3 H3K9me3
Active	Proximal Promoter	H3 and H4 acetylation H3K4me1 H3K9me1 H3K4me3 H2A.Z.
	Enhancer	H3K4me1 H3K27 acetylation

[a] From: Zhou *et al.*, 2011; Rada-Iglesias *et al.*, 2011; Barski *et al.*, 2007; Bernstein *et al.*, 2006; Zentner *et al.*, 2011; Creyghton *et al.*, 2010; Wang *et al.*, 2008; Roh *et al.*, 2006; Hardy *et al.*, 2009; De Gobbi *et al.*, 2011

DMD Fast Forward. Published on February 26, 2016 as DOI: 10.1124/dmd.116.069344
This article has not been copyedited and formatted. The final version may differ from this version.

Table 2: Tissue donor demographics

Fetal Sample ID	EGA[a] (wks)	Sex	% Viability	Postnatal Sample ID	PNA[b] (yrs)	Sex	% Viability
1702f	18	F	69	1816	85.0	M	87
1704f	16	M	56	1807	66.0	F	80
1799f	21	F	98	1812	72.0	F	82
1800f	16	M	97	1813	1.0	M	91
1808f	22	F	93	1833	56.0	M	87
1824f	15	M	90	1834	30.0	F	81
1825f	ND[c]	ND	93	1850	74.0	F	59
1826f	ND[c]	ND	96	1815	1.1	F	90
1827f	17	M	98	1822	3.0	M	91
1832f	13	M	96	1839	5.5	M	71
1836f	ND[c]	ND	98				
1837f	ND[c]	ND	97				
1842f	21	ND	94				
1844f	18	M	96				

[a] EGA = estimated gestational age
[b] PNA = postnatal age
[c] ND = not determined; Although the estimated gestational age was not available, donor was second trimester

DMD Fast Forward. Published on February 26, 2016 as DOI: 10.1124/dmd.116.069344
This article has not been copyedited and formatted. The final version may differ from this version.

Table 3: Fetal and postnatal H3K4me3/H3K27me3 ratios within the *CYP3A4* proximal promoter

Tissue Source	H3K4me3/H3K27me3 Ratio				
	Proximal Promoter Amplicon				**Region**
	1	2	3	4	
Fetal	0.17	0.18	0.03	0.03	**0.10**
Postnatal	1.02	2.42	0.14	0.51	**0.62**

DMD Fast Forward. Published on February 26, 2016 as DOI: 10.1124/dmd.116.069344
This article has not been copyedited and formatted. The final version may differ from this version.

Table 4: Fetal and postnatal H3Ac/H3K27me3 ratios within the *CYP3A4* CLEM4, XREM, and C/EBPβ binding regions

	H3Ac/H3K27me3 Ratio				
Tissue Source	CLEM4 Amplicon				**Region**
	3	5	7	8	
Fetal	0.23	0.45	0.21	0.21	**0.23**
Postnatal	0.70	0.25	0.73	1.19	**0.53**

	H3Ac/H3K27me3 Ratio					
Tissue Source	XREM Amplicon					**Region**
	1	2	3	4	5	
Fetal	0.16	0.09	0.09	1.03	0.61	**0.11**
Postnatal	0.44	0.06	0.05	4.28	0.50	**0.09**

	H3Ac/H3K27me3 Ratio					
Tissue Source	C/EBPβ Amplicon					**Region**
	1	2	4	5	6	
Fetal	0.19	0.10	0.40	0.11	0.26	**0.14**
Postnatal	0.14	0.23	0.36	0.19	0.33	**0.27**

DMD Fast Forward. Published on February 26, 2016 as DOI: 10.1124/dmd.116.069344
This article has not been copyedited and formatted. The final version may differ from this version.

Table 5: Fetal and postnatal H3K4me3/H3K27me3 ratios within the *CYP3A7* proximal promoter

	H3K4me3/H3k27me3 Ratio			
Tissue Source	Proximal Promoter Amplicon			**Region**
	N	L	M	
Fetal	0.36	0.45	0.21	**0.34**
Postnatal	2.89	4.79	3.91	**3.74**

DMD Fast Forward. Published on February 26, 2016 as DOI: 10.1124/dmd.116.069344
This article has not been copyedited and formatted. The final version may differ from this version.

Table 6: Fetal and postnatal H3Ac/H3K27me3 ratios within the *CYP3A7* XREM and C/EBPβ binding regions

	H3Ac/H3K27me3 Ratio			
Tissue Source	XREM Amplicon			**Region**
	A	C	E	
Fetal	0.41	0.22	0.27	**0.27**
Postnatal	9.78	1.79	0.71	**2.71**

	H3Ac/H3K27me3 Ratio				
Tissue Source	C/EBPβ Amplicon				**Region**
	F	G	I	J	
Fetal	0.41	0.16	0.20	0.13	**0.16**
Postnatal	0.17	2.65	1.71	0.42	**0.63**

DMD Fast Forward. Published on February 26, 2016 as DOI: 10.1124/dmd.116.069344
This article has not been copyedited and formatted. The final version may differ from this version.

Figure 1

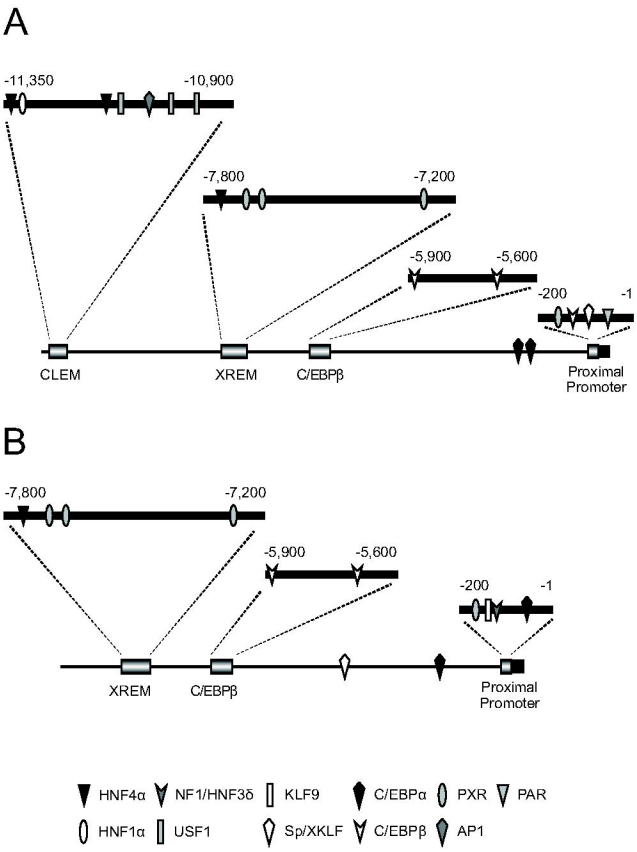

DMD Fast Forward. Published on February 26, 2016 as DOI: 10.1124/dmd.116.069344
This article has not been copyedited and formatted. The final version may differ from this version.

Figure 2

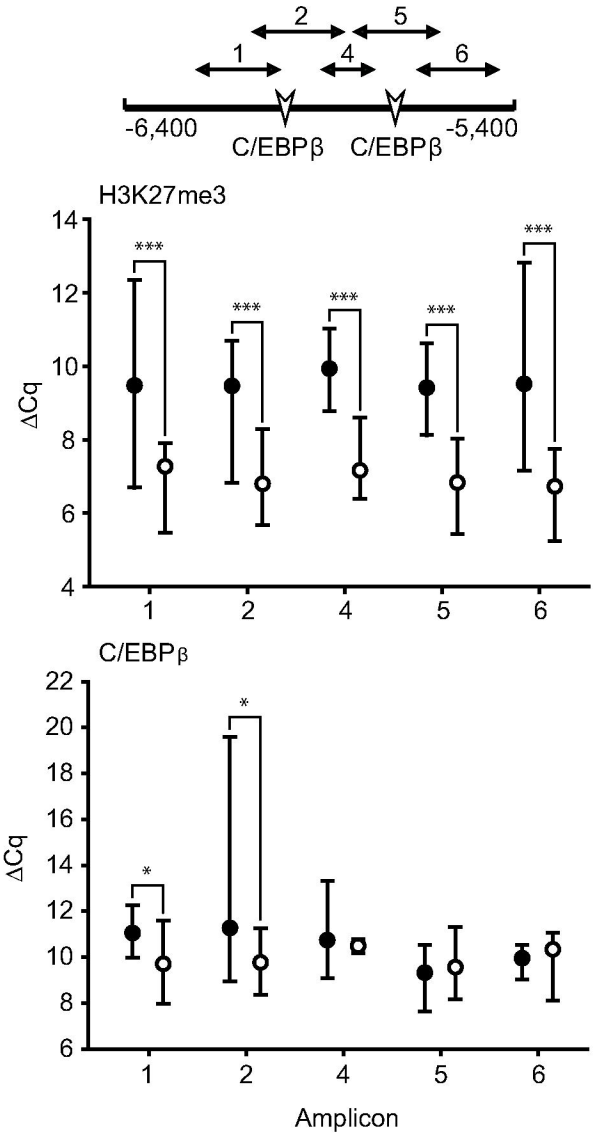

DMD Fast Forward. Published on February 26, 2016 as DOI: 10.1124/dmd.116.069344
This article has not been copyedited and formatted. The final version may differ from this version.

Figure 3

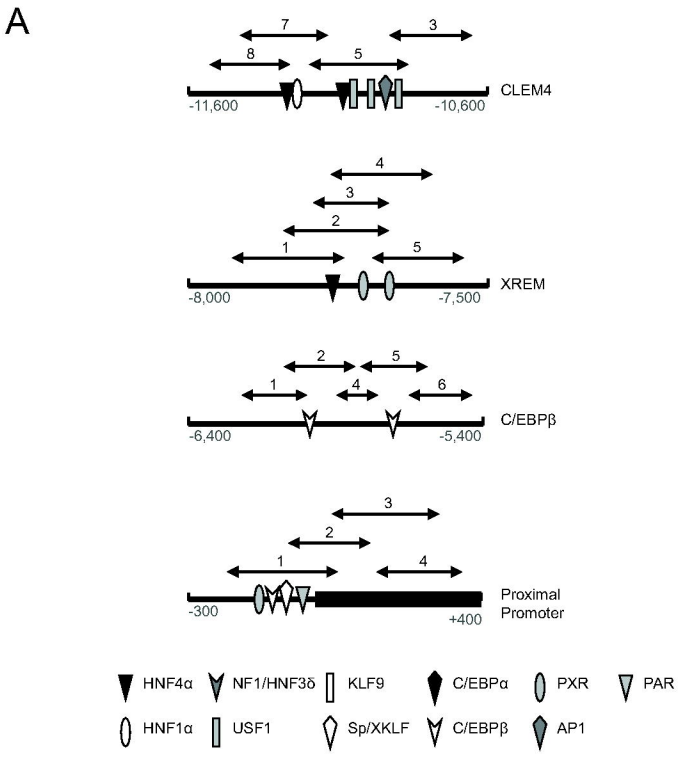

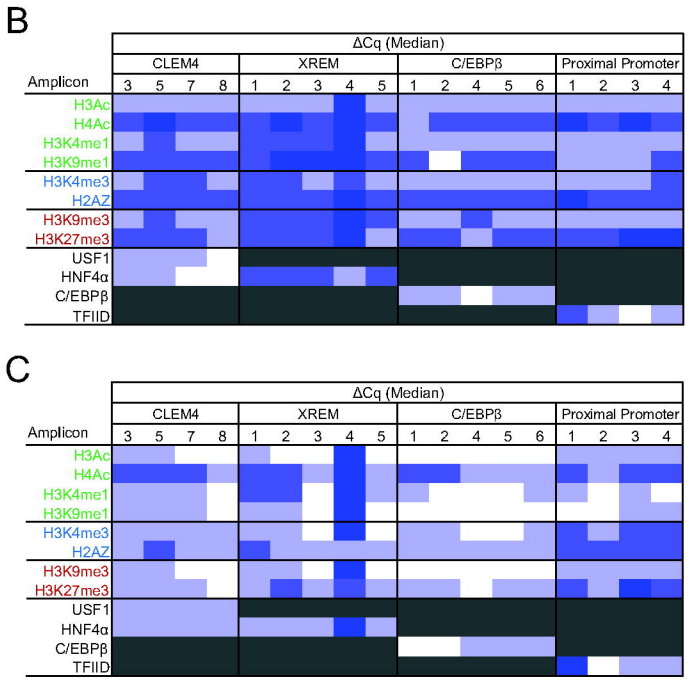

DMD Fast Forward. Published on February 26, 2016 as DOI: 10.1124/dmd.116.069344
This article has not been copyedited and formatted. The final version may differ from this version.

Figure 4

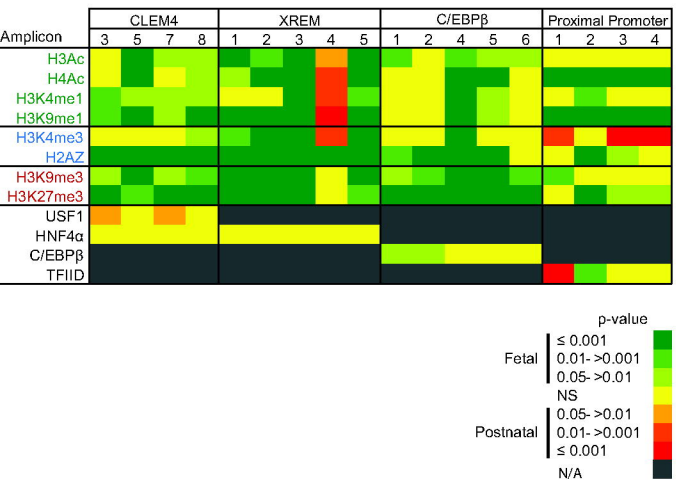

DMD Fast Forward. Published on February 26, 2016 as DOI: 10.1124/dmd.116.069344
This article has not been copyedited and formatted. The final version may differ from this version.

Figure 5

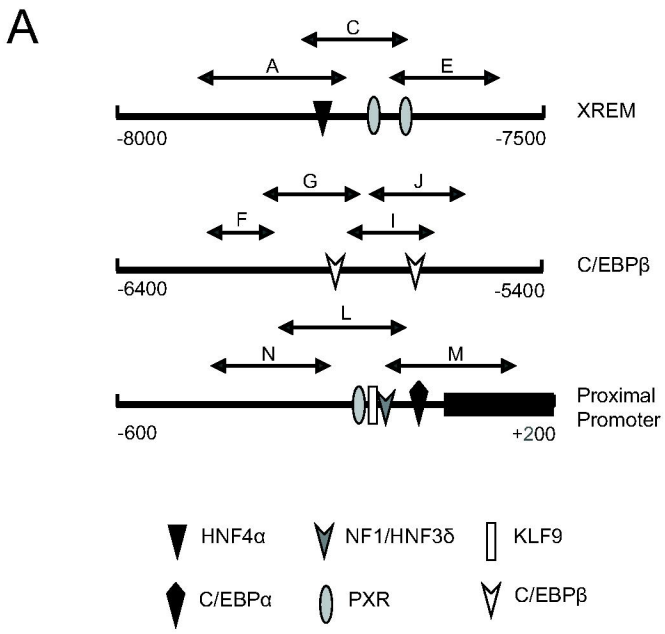

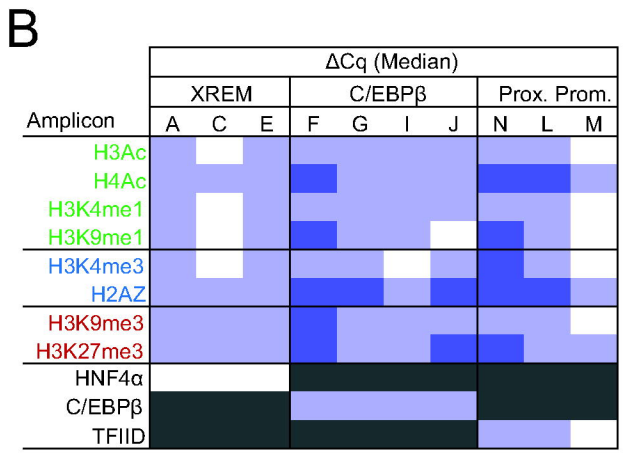

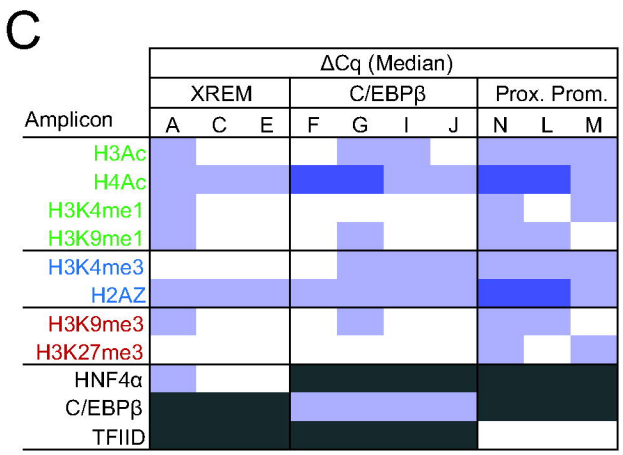

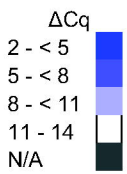

DMD Fast Forward. Published on February 26, 2016 as DOI: 10.1124/dmd.116.069344
This article has not been copyedited and formatted. The final version may differ from this version.

Figure 6

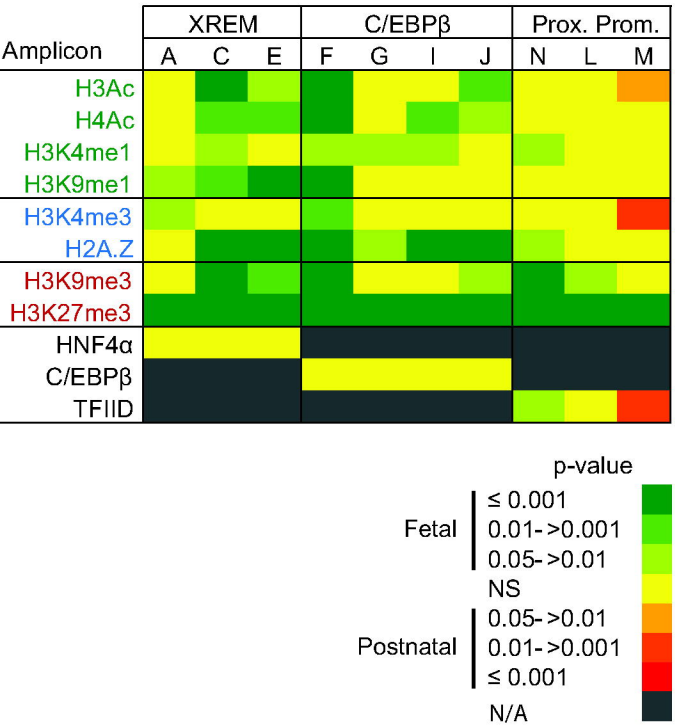

Role of Chromatin Structural Changes in Regulating Human CYP3A Ontogeny

Nicholas L. Giebel, Jeffrey D. Shadley, D. Gail McCarver, Kenneth Dorko, Stephen C. Strom, Ke Yan, Pippa M. Simpson and Ronald N. Hines

Drug Metabolism and Disposition

Supplemental Table 1: qPCR Primers for Quantifying ChIP Products

Element	Amplicon	Forward Primer	Reverse Primer	Size (bps)
		CYP3A4		
CLEM4[1]	8	GCATGTAAGTAGCTGTCTTTCAGG	CCATCTTACTGGCATAATCCTTGTTG	243
	7	CCTAATAATGTGTTTTGGGGTAA	CAAAGCTTCCAAGGTTGCAGAC	272
	5	CTCGTGGTCTGCAACCTTG	TCTGAGCCACAGAGTGACCTA	306
	3	CCAATGCTCCCTTCCGTAGGTCA	GAGTCAGGTACTAGGCTTGGTAAT	251
XREM[2]	1	AGGTCCCCTGGAAAGTCACTG	TTACAAACTGGGCTTTATGAC	182
	2	TGGTTGCTGGTTTATTCTAGAG	ATTTCAAGGGCACCGAGAG	168
	3	AGAAACTCATGTCCCAATTAAAG	ATGATTTCAAGGGCACCGAG	118
	4	GCCCAGTTTGTAAACTGAGATG	ACAGGACAAGGTTTAATAATC	157
	5	GTGCCCTTGAAATCATGTCG	GAATATGATAGCTTGTTCTT	142
C/EBPβ[3]	1	ACCATTTGCTTAAAACATCATGCAC	GCGTCTTGAAAAACATAGATCTTG	198
	2	GAGGGACTGAAGACAAGGAAA	GAAATTAGTGAAGGAAATGAAGATC	216
	4	CATCTCATGATGATCTTCATTTC	AACAGGTAAAAGAGAAATCAGAGAATG	109
	5	CATTCTCTGATTTCTCTTTTACC	GCTGGTTGTGACCACGAAAACG	195
	6	TAGGATGCACATGTCGTTTTCGT	TGCTGTGATTACAAATTGTGCCGGTA	189
Proximal Promoter	1	GATTGAGTTGTTTATGATAC	CTCTTTGCTGGGCTATGTG	248
	2	GCCCTGCCTCCTTCTCTAGC	TCTGGGATGAGAGCCATCAC	170
	3	CACAGAGCTGAAAGGAAGAC	ACGCCCGGCCTGAACATC	235
	4	GGTGCTCCTCTATCTGT	GGCAGTCCACTTGCCTTA	182

Element	Amplicon	Forward Primer	Reverse Primer	Size (bps)
		CYP3A7		
XREM[2]	A	CCTGGAAAGTCACAGGATTTGG	TTATCTCAGTTTACAAACTGGAGTTTATG	177
	C	CAATGAAACTCATGTCCCAACTAAAG	TGATTTCAAGGGCACTGAGAGG	120
	E	CAGTGCCCTTGAAATCATGTCAG	CTTGTCAGAAGTCCAGCTTGTG	127
C/EBPβ[3]	F	CACCGTGTACAGTTGGAGAAGTG	GCTTCAGTCCCTGCAACTGTTC	140
	G	CAGGGACTGAAGCCAAGGAAG	CAGGAAATTGGTGAAGGAAATGAAGATTG	215
	I	CTTCACCAATTTCCTGTTTCATTAATTC	GAGCTCATGTTTCAGCAGAAAG	192
	J	GCCTCATATTCTTTGATTTCTCTTTTAC	AAATGCTACAGAGCTGGTTATGAC	212
Proximal Promoter	N	GCTCTGTCTGGCTGGGTATGAAAG	CCAAGGGTTCTGGGTTCTTATCAC	210
	L	GGACAGCCATAGAGACAAGAGGAGAGTTAATAG	CGTGCTCTGCCTGCAGTCGGAAG	224
	M	CTTCCGACTGCAGGCAGAG	CCAAGTTTGGGATGAGATCCATCACTAC	225

[1] Constitutive Liver Enhancer Module
[2] Xenobiotic Response Enhancer Module
[3] CCAAT-enhancer binding beta domain

Figure 1S: CYP3A4 activity in postnatal primary hepatocyte preparations. CYP3A4 activity was measured for 9/10 of the postnatal samples using a commercial cell-based assay (P450-Glo™ CYP3A4 Assay, Luciferin-IPA; Promega Corporation, Madison, WI, USA) with some modifications, as previously described (Gramignoli *et al.*, 2014). Results are expressed as Luminescent Counting Unit (LCU)/min and are normalized to a million viable cells. The horizontal bar depicts the mean activity determined in 75 different primary human hepatocyte preparations while the shaded area depicts one standard deviation from the mean (Gramignoli *et al.*, 2014). Pediatric (<18 yrs of age) (○) and adult (>18 yrs of age) (●) activities are shown and are labeled with the sample ID numbers (Table 2).